

RESEARCH ARTICLE

10.1002/2013WR013714

Key Points:

- Temporal observations of variability help explain ambiguous correlations
- Interaction between differential accumulation and ablation controls snow distribution

Correspondence to:

J. P. McNamara,
jmcnamar@boisestate.edu

Citation:

Anderson, B. T., J. P. McNamara, H.-P. Marshall, and A. N. Flores (2014), Insights into the physical processes controlling correlations between snow distribution and terrain properties, *Water Resour. Res.*, 50, doi:10.1002/2013WR013714.

Received 19 FEB 2013

Accepted 24 APR 2014

Accepted article online 28 APR 2014

Insights into the physical processes controlling correlations between snow distribution and terrain properties

Brian T. Anderson¹, James P. McNamara², Hans-Peter Marshall², and Alejandro N. Flores²

¹Department of Agriculture, U.S. Forest Service, Idaho City, Idaho, USA, ²Department of Geosciences, Boise State University, Boise, Idaho, USA

Abstract This study investigates causes behind correlations between snow and terrain properties in a 27 km² mountain watershed. Whereas terrain correlations reveal where snow resides, the physical processes responsible for correlations can be ambiguous. We conducted biweekly snow surveys at small transect scales to provide insight into late-season correlations at the basin scale. The evolving parameters of transect variograms reveal the interplay between differential accumulation and differential ablation that is responsible for correlations between snow and terrain properties including elevation, aspect, and canopy density. Elevation-induced differential accumulation imposes a persistent source of variability at the basin scale, but is not sufficient to explain the elevational distribution of snow water equivalent (SWE) on the ground. Differential ablation, with earlier and more frequent ablation at lower elevations, steepens the SWE-elevation gradient through the season. Correlations with aspect are primarily controlled by differences in solar loading. Aspect related redistribution of precipitation by wind, however, is important early in the season. Forested sites hold more snow than nonforested sites at the basin scale due to differences in ablation processes, while open areas within forested sites hold more snow than covered areas due to interception. However, as the season progresses energetic differences between open and covered areas within forested sites cause differences induced by interception to diminish. Results of this study can help determine which accumulation and ablation processes must be represented explicitly and which can be parameterized in models of snow dynamics.

1. Introduction

Mountain snowpacks are highly heterogeneous. Understanding the distribution of water stored as snow on the ground, called snow water equivalent (SWE), is essential for predicting meltwater generation [Clark *et al.*, 2011]. The distribution of SWE, however, can be substantially different than the distribution of snowfall measured by precipitation gauges [Scipi6n *et al.*, 2013]. Methods to estimate where snow resides in mountain watersheds are commonly based on known correlations between SWE and terrain properties including elevation, aspect, slope, and canopy density [Anderton *et al.*, 2004; Dixon *et al.*, 2013; Elder *et al.*, 1991, 1998; Jost *et al.*, 2007; Molotch and Bales, 2005]. The underlying causes of correlations, however, can be ambiguous. For example, correlation between elevation and SWE can be caused by orographic effects producing more precipitation at higher elevations [Houghton, 1979], and by thermal effects producing more snowmelt or rain at lower elevations [Jost *et al.*, 2007; Tarboton *et al.*, 2000]. Correlation between SWE and aspect is commonly explained by differential accumulation on lee and windward slopes [Harrison, 1986], but can also arise from differential ablation due to differences in solar loading on north versus south aspects [Clark *et al.*, 2011; Meromy *et al.*, 2012]. Forest cover can enhance or inhibit both snow accumulation and melt depending on many interacting terrain and climate properties [Lundquist *et al.*, 2013]. Additionally, lateral flow of meltwater within the snowpack [Eiriksson *et al.*, 2013], slope-induced redistribution by avalanching and creep [Kerr *et al.*, 2013], and many other processes can further complicate SWE distribution by adding local variability with correlation lengths between 10 and 100 m [Deems *et al.*, 2008; Shook and Gray, 1998; Trujillo *et al.*, 2007, 2009] to regional trends extending over several kilometers [Gillan *et al.*, 2010].

The spatial distribution of SWE arises from season-long interplay between spatially and temporally heterogeneous snow accumulation and ablation processes [Tarboton *et al.*, 2000]. Clark *et al.* [2011] suggested that snow surveys conducted at an assumed time of maximum accumulation can bias conclusions concerning controls on snow distribution to favor accumulation processes. One-time synoptic snow surveys will reveal only information about the integrated processes responsible for the state of the snowpack up to that

time. The potentially confounding relationships between observed correlations and underlying processes make it difficult, if not impossible, to ascribe causal relationships between basin-wide trends in SWE and particular processes. Knowledge about processes controlling snow distribution, however, is critical for evaluating the performance of snow accumulation and melt models [Blöschl *et al.*, 1991]. Model improvement comes from understanding why models fail rather than just where they fail.

Issues of snowpack heterogeneity are particularly salient in the warm, shallow snowpacks of the midelevation zone in the intermountain Western US. There, changing snow conditions pose significant challenges for water resource management [Hamlet and Lettenmaier, 2007], streamflow dynamics [Luce and Holden, 2009], and upland ecology [Smith *et al.*, 2011]. Midelevation snowpacks can undergo subseasonal cycles of accumulation and ablation, can be subjected to rain-on-snow events, can be spatially discontinuous, and can have a lower elevation limit at a transient snowline [Kormos, 2013]. The concept of a time of maximum snow accumulation has little meaning at watershed scales, as snow accumulation in lower elevations tends to peak earlier than in higher elevations.

The purpose of this paper is to examine the causes leading to correlations between snow and terrain properties in a midelevation watershed characteristic of the intermountain Western United States. Our premise is that the spatial variability of SWE at any time is a product of the relative importance of processes controlling differential accumulation and differential ablation through the season, and that improved understanding about processes controlling variability can be obtained by observing the development of variability through snow accumulation and melt seasons. Snow surveys were conducted in the Dry Creek Experimental Watershed (DCEW) in southwest Idaho, USA through the winters of 2009 and 2010 at various spatial and temporal scales to identify correlations between snowpack and terrain properties, and to track the evolution of snowpack variability leading to observed correlations. Snow surveys included: (1) synoptic maximum accumulation surveys over multiple 50–100 m scale transects distributed by elevation and aspect in the snow-covered portion of the 27 km² basin in both years, (2) repeated surveys through the 2010 season over a 1 km² grid in a forested portion of the watershed, and (3) repeated surveys through the 2010 season over three transects at low, mid, and high elevation sites in the snow-covered area. Standard correlation methods are used to identify relationships between snow properties and terrain properties at grid and basin scales. Variograms of transect surveys are used to understand the changing scales of variability throughout the snow accumulation and ablation seasons.

2. Study Site and Hydrometeorological Setting

The Dry Creek Experimental Watershed (DCEW) drains 27 km² in a dominantly southwest facing, semiarid mountain front basin in the foothills north of Boise, Idaho (Figure 1a). Elevations within DCEW range from 950 m at the lower stream gage to 2130 m at the highest summit. During the study period, three stations within the watershed collected standard meteorological data at elevations of 1100 m (Lower Weather), 1610 m (Treeline), and 1850 m (Lower Deer Point). In addition, there is a Snow Telemetry station (SNOTEL) operated by the US Natural Resources Conservation Service (NRCS) outside DCEW at the adjacent Bogus Basin Ski Resort at 1932 m.

Annual average precipitation increases from approximately 400 mm at the Lower Weather meteorological station to approximately 900 mm at the Bogus Basin SNOTEL station [Aishlin and McNamara, 2011]. The lower elevations within the watershed receive occasional snow that usually does not last more than a few days or weeks, while higher elevations are generally snow-covered from early December to mid-May. The elevation above, which persistent winter-long snow occurs, is typically around 1500 m.

Slopes are steep and aspects are highly variable, although the upper elevations of the basin generally face south. Vegetation is predominantly sagebrush (*Artemisia tridentata*), bitterbrush (*Prushia tridentata*), mixed grasses, and a variety of riparian vegetation at lower elevations. Higher elevations contain forested areas composed mostly of Douglas Fir (*Pseudotsuga menziesii*), Ponderosa Pine (*Pinus ponderosa*), Green Alder (*Alnus viridis*), and Ceanothus (*Ceanothus americanus*). Portions of the higher elevation regions were selectively logged in the 1970s.

Winter precipitation (October 1 to April 30) amounts in 2009 and 2010 were relatively similar (Figure 2), and increased with elevation by approximately 44 mm/100 m. The snow course at the Bogus Basin SNOTEL site

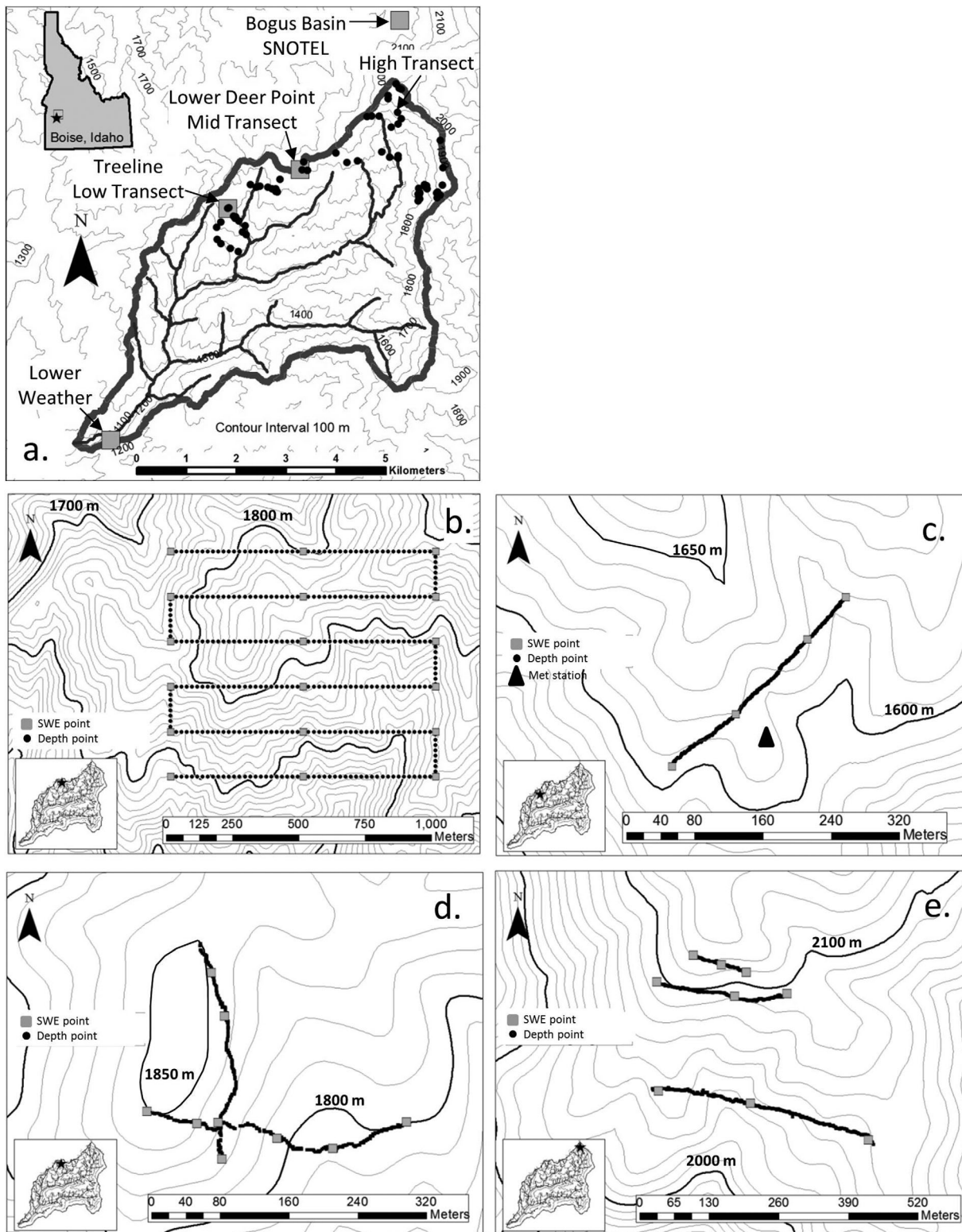


Figure 1. (a) Dry Creek Experimental Watershed in southwest Idaho with locations of meteorological stations (gray squares), biweekly surveys (Low Transect, Mid Transect, High Transect), and synoptic surveys (black dots). (b) Lower Deer Point grid (LDP grid). (c) Low Transect site within the Treeline Watershed. (d) Mid Transect site within the LDP grid. (e) High Transect site.

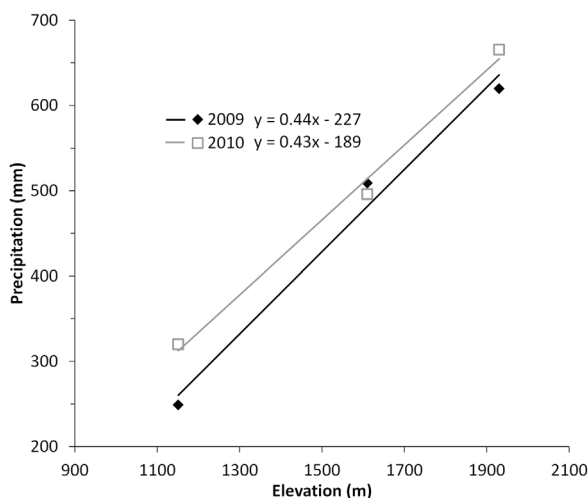


Figure 2. Winter precipitation (October 1 to April 30) at Lower Weather, Treeline, and Bogus Basin meteorological stations.

reported April 1st SWE measurements that were 90% and 88% of the 1971–2000 average for the 2009 and 2010 water years, respectively. A NRCS snow course near the Low Transect (Figure 1a) reported March 1st SWE measurements of 45% (2009) and 156% (2010) of the 1971–2000 average, while April 1st measurements showed 126% (2009) and 56% (2010). During both years, DCEW experienced significant snowfall events later in the season after significant ablation had occurred.

3. Methods

3.1. Snow Measurements

Snow depth, snow density, and SWE were measured at points described in section 3.2. SWE was measured with a “Federal” or “Mt. Rose” snow sampler according to the specifications designed by the NRCS and described in *Gray and Male* [1981]. Due to the uncertainties in sampling shallow snow (<30 cm) with a Federal sampler, a 12 in. long 3 in. diameter plastic snow tube, with a small, calibrated scale (*Snowmetrics*) was used in these conditions. At each SWE measurement point, snow depth was measured on the outside of the sampler, and snow density relative to the density of water was determined by dividing SWE depth by snow depth.

Snow depth, snow density, and SWE

Where SWE was not measured, snow depth at individual points was measured using an incremented probe inserted vertically into the snowpack. During the 2010 snow season, an automatic recording snow depth instrument (*MagnaProbe, SnowHydro*; Sturm, M. and J. Holmgren, 1997, Patent number 5864059) was used. The *MagnaProbe* uses a magnetic position sensor attached to a 12 in. diameter plastic basket that slides along a steel rod and remains at the snow surface while the rod is inserted through the snow to the ground. The height of the basket (i.e., snow depth) and GPS location of the sample site are recorded on a Campbell Scientific, Inc. CR800 datalogger. The device allows orders of magnitude more measurements than standard depth measurement methods.

3.2. Sampling Strategy

Measurements at three scales were performed (Figure 1). First, basin-wide synoptic surveys were conducted in March 2009 and March 2010, the assumed time of maximum accumulation in the higher elevations, over the snow-covered area. Second, a 1000 m × 800 m grid was surveyed four times in 2010. Third, three transects at low, mid, and high elevation sites in the snow-covered area were surveyed five to nine times in 2010 (see Table 1 for dates).

The basin-wide synoptic surveys consisted of 35 sites selected to represent elevation, aspect, and vegetation classes in the DCEW (Figure 1a) [Shallcross, 2011]. At each site, snow depth measurements were made at 2 m spacing along transects approximately 50 m long and perpendicular to the slope. SWE was measured at endpoints and midpoints of each transect.

A 1000 m × 800 m grid with approximately 200 m of relief surrounding the Lower Deer Point (LDP) meteorological station at 1850 m elevation was measured using a gridded sampling pattern (Figure 1b). The grid is aligned with a pixel in the Snow Data Assimilation System (SNODAS) of the US National Weather Service [Carroll et al., 2006], and also overlaps with an area that was used to evaluate the fractional snow cover product of the Moderate Resolution Imaging Spectroradiometer (MODIS) generated by NASA [Homan et al., 2011]. A comparison of snow accumulation and melt in the grid is qualitatively compared to SNODAS output (section 5). A comprehensive model evaluation, however, is beyond the scope of this paper. The gridded sampling pattern includes a variety of vegetation types and densities, slopes, and aspects. The

Table 1. Snow Depth, Density and Water Equivalent for Transect, Grid, and Basin Surveys

Location/Date	Snow Depth				Snow Density				Snow Water Equivalent (SWE)		
	Mean (cm)	n	stdev (cm)	CV	Mean (kg/m ³)	n	stdv (kg/m ³)	CV	Mean (cm)	stdv (cm)	CV
<i>Treeline Transect</i>											
23 Dec 2009	31	299	7	0.23	213	3	10	0.05	7	1	0.22
7 Jan 2010	39	728	9	0.23	276	3	9	0.03	11	2	0.22
19 Jan 2010	29	302	14	0.48	322	3	9	0.03	9	4	0.48
10 Feb 2010	32	704	19	0.59	318	6	20	0.06	10	6	0.59
3 Mar 2010	21	687	21	1.00	363	6	17	0.05	8	8	1.00
16 Mar 2010	11	703	19	1.73	385	5	23	0.06	4	7	1.73
<i>Lower Deer Point Transect</i>											
23 Dec 2009	50	202	22	0.44	185	2	15	0.08	9	4	0.44
7 Jan 2010	56	451	11	0.20	211	2	14	0.07	12	2	0.20
22 Jan 2010	66	600	16	0.24	301	2	44	0.15	20	7	0.37
5 Feb 2010	85	621	18	0.21	298	8	22	0.07	25	6	0.23
26 Feb 2010	90	632	18	0.20	289	4	31	0.11	26	7	0.27
12 Mar 2010	78	676	18	0.23	352	9	21	0.06	27	6	0.23
1 Apr 2010	81	618	24	0.30	364	4	16	0.04	29	9	0.30
15 Apr 2010	72	618	23	0.32	400	8	26	0.07	29	10	0.33
23 Apr 2010	26	390	24	0.92	419	5	60	0.14	11	10	0.91
<i>Upper Dry Creek Transect</i>											
8 Jan 2010	80	687	14	0.18	275	12	30	0.11	22	5	0.20
29 Jan 2010	106	847	21	0.20	302	16	31	0.10	32	7	0.22
5 Mar 2010	120	818	19	0.16	384	10	31	0.08	46	8	0.18
14 Apr 2010	130	672	25	0.19	405	8	17	0.04	53	11	0.20
2 May 2010	75	649	25	0.33	358	9	91	0.25	27	11	0.42
<i>Lower Deer Point Grid</i>											
15 Jan 2010	56	303	20	0.36	286	18	37	0.13	16	6	0.39
19 Feb 2010	78	1705	25	0.32	308	18	35	0.11	24	8	0.34
22 Mar 2010	57	1705	35	0.61	356	16	61	0.17	20	13	0.65
16 Apr 2010	53	1705	39	0.74	422	18	57	0.14	22	17	0.75
<i>Basin</i>											
20 Mar 2009	76	846	35	0.46	375	103	74	0.20	29	13	0.45
21 Mar 2010	71	642	44	0.62	379	44	71	0.19	27	17	0.63

northern portions of the grid are higher and more north facing, while the southern portions of the grid are lower in elevation and more south facing. Measurements were made in six E-W 1000 m transects, separated by 160 m each. Depth was measured every 20 m in each transect (51 points) and in N-S lines connecting alternating ends of each E-W transect (seven points) for a total of 341 points. The mean of five depth measurements at each of the 341 points was assigned to that point. SWE was measured at the ends and mid-points of each E-W transect. At each point, five depth measurements were made in a cross pattern for a total of 1705 measurements. The first survey on 15 January 2010, however included only one depth measurement per point and did not include N-S connecting transects.

Three transects for frequent measurements were selected at low, mid, and high elevation sites, henceforth called Low Transect, Mid Transect, and High Transect. Depth was measured at 1 m spacing in each transect. Actual transect lengths varied among sites (Figures 1c–1e and Table 1). Each site is associated with a dominant process mechanism that exerts control on the distribution of snow cover and SWE during the accumulation and ablation seasons. Low Transect traversed the Treeline Watershed on northeast and southwest aspects for approximately 300 m to capture the aspect and slope differences of opposing hillslopes (Figure 1c). The Treeline Watershed is a 0.02 km² instrumented subbasin with a meteorological station at 1610 m elevation that lies in a sagebrush steppe ecotone transitioning to higher elevation mixed conifer forest. Snow cover at Treeline Watershed is often shallow, patchy, and variable from year to year. Precipitation can be variable, with some years receiving more rain than snow, and vice versa. Topography includes steep opposing hillslopes that show the same snow spatial patterns from year to year. Snow tends to melt out quickly on the southwest aspect and remains throughout the season on the northeast aspect [Williams *et al.*, 2009]. Additionally, hourly time-lapse photographs were taken at Treeline Watershed with a waterproof handheld digital camera (Pentax Optio WS 80) mounted on the post of a precipitation gauge facing north with the two predominant aspects visible. Mid Transect site consisted of two 300 m transects (Figure 1d)

aligned N-S and E-W, to include a range of forest canopy, slope, and aspect found in the vicinity of the Lower Deer Point meteorological station. High Transect at 2100 m elevation consisted of three transects along elevation contours 100, 250, and 500 m long (Figure 1e). High Transect, located at the top of the watershed, is not a long-term study site, but was selected for snow surveys specifically for this study. The site contains scattered conifer trees, and ceanothus and alder shrubs and holds the deepest, most persistent snowpack throughout the basin. Measurements at all three transect sites were performed approximately biweekly in 2010.

3.3. Statistical Analyses

3.3.1. Correlations Between Snow Depth and Terrain Properties at Basin and Grid Scales

Pearson's correlation coefficients were calculated between snow depth and several topographic and vegetation variables for the basin-wide, grid, and transect surveys. For the basin-wide surveys, a mean snow depth for each of the 35 transects was assigned to the center point of each transect. For the grid surveys, the mean of the five snow depth measurements at each of the 341 points was used. For the transect surveys, single point snow depth measurements were used. Correlations were evaluated for elevation, aspect, slope, northness, canopy density, and wind exposure index (WEI). Elevation and canopy density were not evaluated at transect scales due to limited elevation ranges and low spatial resolution (30 m) of canopy density data.

Elevation, aspect, and slope for each point were obtained from a LiDAR-derived digital elevation model (DEM) with a resolution of 1 m [Shallcross, 2011]. Aspect values (0–360°) were transformed using the cosine function to correspond with north (1) and south (–1). Northness was calculated to represent the influence of solar radiation by combining slope and aspect [Molotch and Bales, 2005; Veatch et al., 2009]. Northness ranges from –0.5 to 0.5 where steeper, more south facing slopes are closer to –0.5 and flatter, north facing slopes are closer to 0.5. A directional wind exposure index (WEI) was calculated from the DEM based on the approach of Lapen and Martz [1993] and Anderton et al. [2004]. The wind exposure index was calculated by first estimating the average elevation within a 35 m radius wedge-shaped region extending in a specified direction associated with a dominant wind direction from the cell of interest, and then subtracting this elevation value from the elevation field. We used an azimuth range of 270–360° to correspond with the dominant winter wind direction in the study area. The result is a raster data set that is negative for areas sheltered by upwind topography and positive for areas exposed to wind. Canopy density values were obtained from the National Land Cover Dataset (NLCD) [Homer et al., 2012]. NLCD is at 30 m resolution and derived from Landsat data.

3.3.2. Variograms of Snow Depth at High Resolution Transect Sites

Variograms of snow depth were constructed for Low Transect, Mid Transect, and High Transect following methods described by Webster and Oliver [2001]. Variance at lag spacing, h , within a transect is calculated as

$$\gamma(h) = \left(\frac{1}{2N(h)} \right) \cdot \sum_{i=1}^{N(h)} (z_i - z_{i+h})^2 \quad (1)$$

where N is the number of pairs of points at a given lag spacing and z is snow depth. Variograms are constructed by plotting variance against lag spacing. Characteristics of an empirical variogram are commonly described by fitting a model to the data. A spherical variogram model showed the best fit to our data, defined as

$$\gamma(h) = \begin{cases} c \left\{ \frac{3h}{2a} + \frac{1}{2} \left(\frac{h}{a} \right)^3 \right\} & \text{for } h \leq a, \\ c & \text{for } h > a, \end{cases} \quad (2)$$

where c is the sill variance and a is the range. Variogram estimates are highly uncertain when the number of pairs of points at a given lag is <150 [Webster and Oliver, 2001]. Because the *MagnaProbe* allowed many more depth measurements to be performed, a Monte Carlo technique was used to produce robust estimates of variance and their uncertainty. The same number of observations as the original data set was sampled randomly

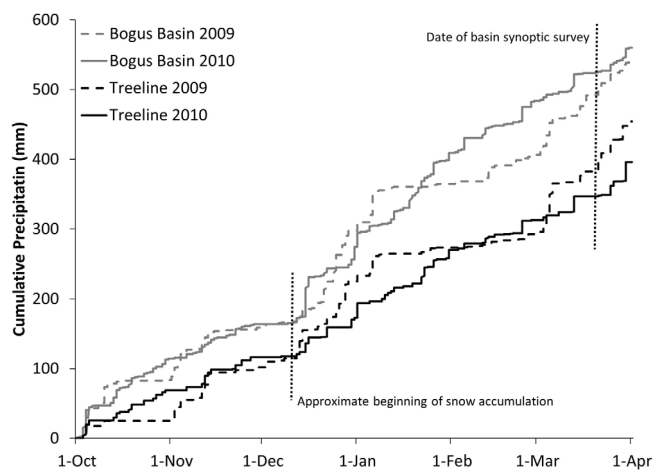


Figure 3. Cumulative precipitation at Treeline meteorological station and Bogus Basin SNOTEL station in winter 2009 and 2010.

with replacement, the variogram and best-fit model parameters calculated, for 50 different random samples. Quantiles of model parameters at 5%, 50%, and 95% were calculated.

4. Results

In the remainder of this paper, the terms precipitation and snowfall refer to water collected in weighing bucket gauges at meteorological stations (Figure 1). Precipitation is the depth of water as rain and snow, snowfall refers to precipitation that fell as snow. The term SWE refers to the snow water equivalent on the ground at survey locations.

4.1. Precipitation in the Snow-Covered Area

A persistent snow line developed in mid-December below the Treeline Watershed at approximately 1500 m elevation in both 2009 and 2010. The Lower Weather meteorological station received some snow in January, but precipitation there fell primarily as rain. At the Treeline and Bogus Basin meteorological stations, precipitation between October 1 and mid-December each year fell primarily as rain. Cumulative precipitation in mid-December was surprisingly similar each year for both sites (Figure 3). The cumulative precipitation gradient between the Treeline meteorological station and the Bogus Basin SNOTEL station on the date of the basin survey each year was 18 mm/100 m and 40 mm/100 m in 2009 and 2010, respectively (derived from Figure 3).

4.2. Snow on the Ground

4.2.1. Basin Synoptic Survey

Mean snow depth, snow density, and SWE were similar in the late March surveys in 2009 and 2010 (Table 1). The coefficient of variation (CV) each year shows that snow depth was much more variable than snow density (Table 1). Elevation had the strongest positive correlation with snow depth during both years followed by aspect in 2009 and canopy density in 2010 (Table 2) indicating that deeper snow occurs at higher elevations, on northerly aspects, and in dense canopies. WEI was negatively correlated with snow depth in both years indicating that areas sheltered from Northwest winds hold more snow than exposed areas. Correlations between snow depth and all variables except slope were generally stronger in 2010, likely due to a snowstorm prior to the survey in 2009.

Within the elevation range of the surveys, which spanned most of the snow-covered area, SWE increased with elevation by 53 mm/100 m and 63 mm/100 m in 2009 and 2010, respectively (Figure 4). The gradients, however, were influenced by low SWE values below approximately 1750 m elevation. At higher elevations the SWE-elevation gradients were considerably lower at 22 mm/100 m and 8 mm/100 m (not shown). Snow density did not change significantly with elevation (data not shown), suggesting that the SWE trends in Figure 4 are controlled by snow depth.

4.2.2. Grid Surveys

The LDP grid was measured four times in 2010. Correlations between snow depth and physiographic variables were similar as reported at the basin scale. Elevation was generally the strongest correlate with snow depth, although on 16 April 2010 correlation with northness exceeded all others (Table 2). Canopy density had the lowest correlations with snow depth in the early season, but increased later in the season. WEI was negatively correlated with snow depth. Mean snow depth was greatest in mid-February (Figure 5 and Table 1), while deepest individual snow values were encountered during the final survey in April (Figure 6). Little ablation had occurred during January and February, while the March and April surveys indicate significant melt had occurred along the low elevation, southern portions of the grid. Average density increased through the

Table 2. Snow Depth Correlation Coefficients ($\alpha=0.01$)^a

Date	n	Elevation [m]	Aspect	Slope	Northness	Canopy Density	Wind Exposure Index
<i>Low Transect</i>							
12/23/2009	299		0.43	0.12	0.17		0.06
1/7/2010	332		0.26	0.14	0.27		-0.12
1/19/2010	302		0.66	0.15	0.66		-0.48
2/10/2010	307		0.76	NSS	0.76		-0.48
3/3/2010	332		0.79	0.16	0.78		-0.42
3/16/2010	308		0.85	-0.75	0.83		-0.6
<i>Mid Transect</i>							
12/23/2009	202		NSS	0.36	-0.17		0.25
1/7/2010	452		NSS	0.15	NSS		NSS
1/22/2010	600		0.28	0.36	0.22		-0.21
2/5/2010	622		0.32	-0.06	0.2		-0.2
2/26/2010	632		0.27	-0.08	0.19		-0.21
3/10/2010	676		0.39	-0.03	0.29		-0.28
4/1/2010	619		0.38	NSS	NSS		-0.46
4/15/2010	619		0.42	-0.11	0.39		-0.37
4/23/2010	390		0.45	-0.1	0.36		-0.33
<i>High Transect</i>							
1/8/2010	687		0.36	-0.47	0.49		0.45
1/29/2010	847		0.3	-0.53	0.54		0.33
3/5/2010	818		0.37	-0.44	0.47		NSS
4/14/2010	672		0.28	-0.42	0.43		0.17
5/2/2010	649		0.42	-0.58	0.6		0.34
<i>Lower Deer Point Grid (LDP GRID)</i>							
1/15/2010	303	0.45	0.4	-0.17	0.41	0.16	-0.41
2/19/2010	1725	0.42	0.38	-0.14	0.38	0.14	-0.39
3/22/2010	1725	0.47	0.39	-0.22	0.4	0.23	-0.38
4/16/2010	1725	0.42	0.48	-0.22	0.5	0.34	-0.5
<i>Basin</i>							
2009	846	0.57	0.18	-0.12	0.2	0.32	-0.27
2010	642	0.68	0.36	0.09	0.42	0.44	-0.44

^aNSS, not statistically significant.

season from 286 to 402 kg/m³. The two lower elevation southern-most transects of the grid showed significant snow-free portions by mid-March, while the more north facing, higher elevation transects near the northern edge of the study site contained the deepest snow and continued to accumulate snow up to the final survey in April.

4.2.3. Transect Surveys

Comparison of mean snow depth, snow density, and SWE at Low Transect, Mid Transect, and High Transect confirm that elevation is a strong control on snow depth at the watershed scale (Figure 7 and Table 1). The effect of elevation is established early in the accumulation season. As lower elevations experience ablation, differences in snow depth across elevations increase. Snow density trends are similar for each site and are relatively consistent across elevations.

Maximum accumulation at Low Transect occurred in mid-January (Figure 7 and Table 1). Complete melt occurred in late March, and several additional storms deposited snow during late April. Aspect, northness, and WEI all showed increasing correlations with snow depth through the season (Table 2). Variations in snow depth across Low Transect in December and early January were small (Figure 8). However, from mid-January through complete melt in March, large variations in snow depth occurred between the northeast and southwest aspects (Figures 8 and 9).

Maximum SWE accumulation at Mid Transect occurred in mid-April, although it had remained relatively stable since late February (Figure 7 and Table 1). Variations in snow depth related to canopy density were apparent (Figure 10); however, we do not report correlations due to differences in resolution of snow depth measurements (1 m) and canopy density information (30 m). In Figure 10, snow depths within the Mid Transect with NLCD canopy density values above and below 60% are highlighted. The value 60% was chosen based on observations by Veatch *et al.* [2009] who showed that snow under moderate canopy densities tends to be deepest. Throughout the season, areas under low canopy density held more snow than areas under high canopy density, although the differences become less visually apparent later in the season. Aspect was not

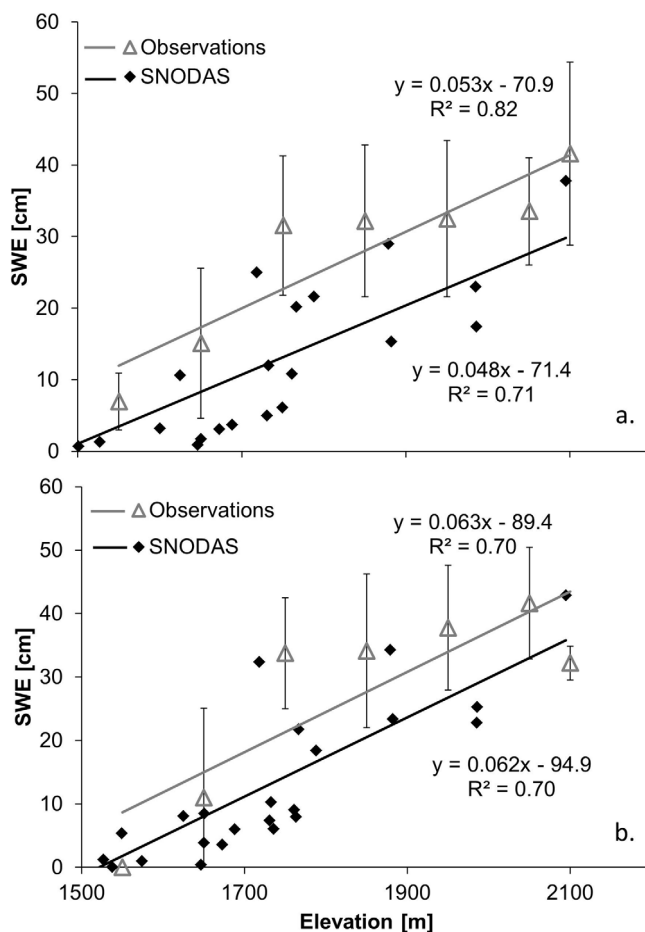


Figure 4. Basin-wide snow survey results and SNODAS model predictions for all model pixels covering DCEW for (a) 16–18 March 2009 and (b) 21 March 2010. Observations are averaged over 100 m elevation bins. Error bars are 1 standard deviation centered on the average.

separations during accumulation and ablation seasons, with the most significant increase occurring when significant ablation begins. The increase in the sill is most evident at Low Transect (Figure 11a) where January surveys show relatively low variances compared to February and March surveys. To assess if the increase in variance during accumulation was due to an increase in relative variability or just that snow depths were increasing causing differences to increase, we plotted the percent variability relative to the mean at each lag (Figures 11d–11f). This is calculated as the pairwise relative variance, henceforth called relative variability, where each point pair difference is divided by the mean value of the two points, and then averaged. The relative variability ranged between 20% and 30% during the accumulation period for all sites, and significantly increased during ablation. Mid Transect and High Transect surveys increased to 40–50% relative variability, whereas Low Transect relative variability increased to 160%. The very high relative variabilities occur when snow-free areas appear.

The range at Low Transect increased in the early season from 12 to 53 m before declining to values that roughly correspond with the length scale of the snow patches that develop on the NE facing hillslopes. Significant variability at <1 m is indicated by the nugget values in all but the final sampling event, which had many snow free locations. At the Mid Transect, early season ranges increased from 66 to 132 m before decreasing to approximately 22 m after significant melt began. Note the significant hole effect in the final two survey variograms (Figure 11b), which occurs at length scales >20 m. High Transect range values have large uncertainties, but show a similar pattern of decreasing correlation length throughout accumulation and melt. High Transect nugget values are more than twice as large as surveys at the other sites at similar times, illustrating the under sampling in this highly variable location.

significantly correlated with snow depth early in the season. Beginning in late-January, aspect was significant and increased through the season. WEI correlation trends were similar to aspect, although negative.

Snow depth at the High Transect increased until maximum accumulation in mid-April (Figure 7 and Table 1). High Transect held the deepest snowpack of all sites and the greatest range in values at the transect scale, with snow depth variations of >150 cm within 10 m. Cornices and drifts were observed in the upper portions of the basin near ridges. Correlations with snow depth and all variables were significant on most dates. Trends through the season, however, were not as apparent as at other sites. Unlike other sites WEI had a relatively high correlation early in the season compared to other sites.

4.3. Variograms

Variograms for each transect site have some common characteristics (Figure 11 and Table 3). Foremost, the sill, which can be considered the variance, increases with time for all lag

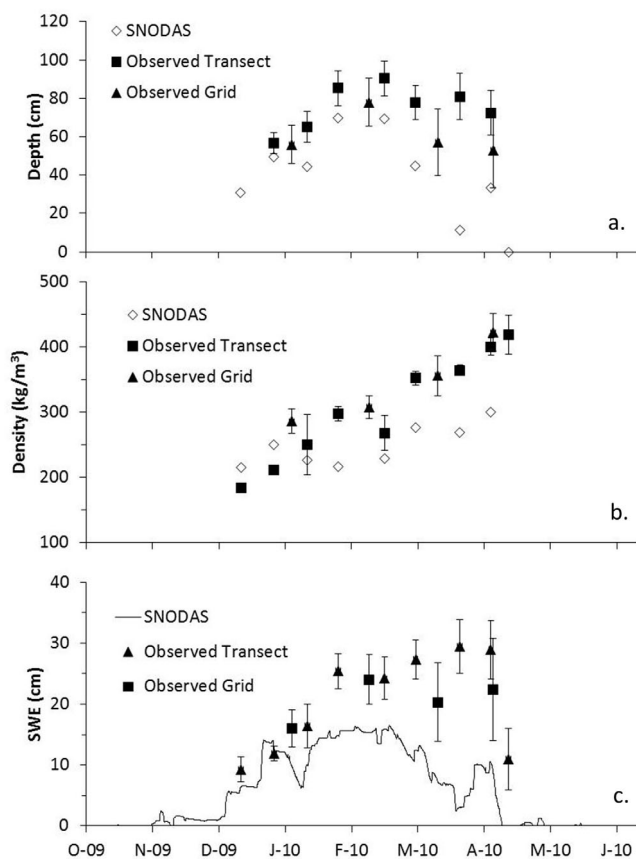


Figure 5. Snow survey results and SNODAS predictions for the LDP grid (a) depth, (b) density, and (c) SWE with daily SNODAS predictions displayed as a continuous line for clarity. Error bars on survey results indicate 1 standard deviation.

itation phase and snowmelt rates. Although the precipitation-elevation gradient is significant, the steep SWE-elevation gradient (Figure 4) confirms that elevation-induced precipitation variability is not sufficient alone to explain the relationship between elevation and late-season SWE on the ground. Another process must be important, for example, elevation control on snowmelt rates due to air temperature effects, as was found in a study conducted in a snow-dominated watershed of similar relief in British Columbia, Canada [Jost *et al.*, 2007].

The evolving differences between the precipitation-elevation gradient and the SWE-elevation gradient (Figure 12) illustrate the relative importance of elevation-induced differential accumulation and ablation. Early in the season, the two gradients are similar, approximately 11 mm/100 m in mid-December, suggesting that elevation-induced precipitation differences dictate basin scale SWE variability. However, as the season progresses, the cumulative precipitation and SWE gradients diverge. The precipitation-elevation gradient gradually increases through the season to approximately 40 mm/100 m. The SWE-elevation gradient increases similarly in February, but increases steeply in late January and then again in March through April. Precipitation at the Treeline meteorological station during those periods fell primarily as snow, suggesting that the steep SWE-elevation gradient was due to ablation at low elevations.

5.2. Aspect

Aspect affects insolation, local wind, vegetation, and slope, all of which exert some control on snow accumulation and ablation. Consequently, different snow accumulation and melt processes can lead to similar snow distribution patterns, complicating interpretation of statistical relationships. Correlations at the LDP grid illustrate this point. An increase (inverse) in correlation with the wind exposure index (WEI) from -0.38 on 22 March 2010 to -0.5 on 12 April 2010 occurred during a period when the SWE-elevation gradient on the ground increased much more than did the precipitation-elevation gradient (Figure 12). This suggests

5. Discussion

Correlations between snow and terrain properties arise from the interplay between differential accumulation and differential ablation of snow across spatial and temporal scales. Understanding causes of correlations is challenging because many processes controlling snow distribution are affected by some common terrain properties, which can both increase and decrease the amount of snow depending on the dominant process. Here we use observations on the evolution of snow variability through accumulation and ablation seasons to explain late-season relationships between snow distribution and the following terrain properties: elevation, aspect, and canopy cover.

5.1. Elevation

Elevation imprints a persistent source of variability in SWE at the basin scale (Figures 4 and 7) due to orographic effects on precipitation magnitude (Figure 3), and air temperature effects on precip-

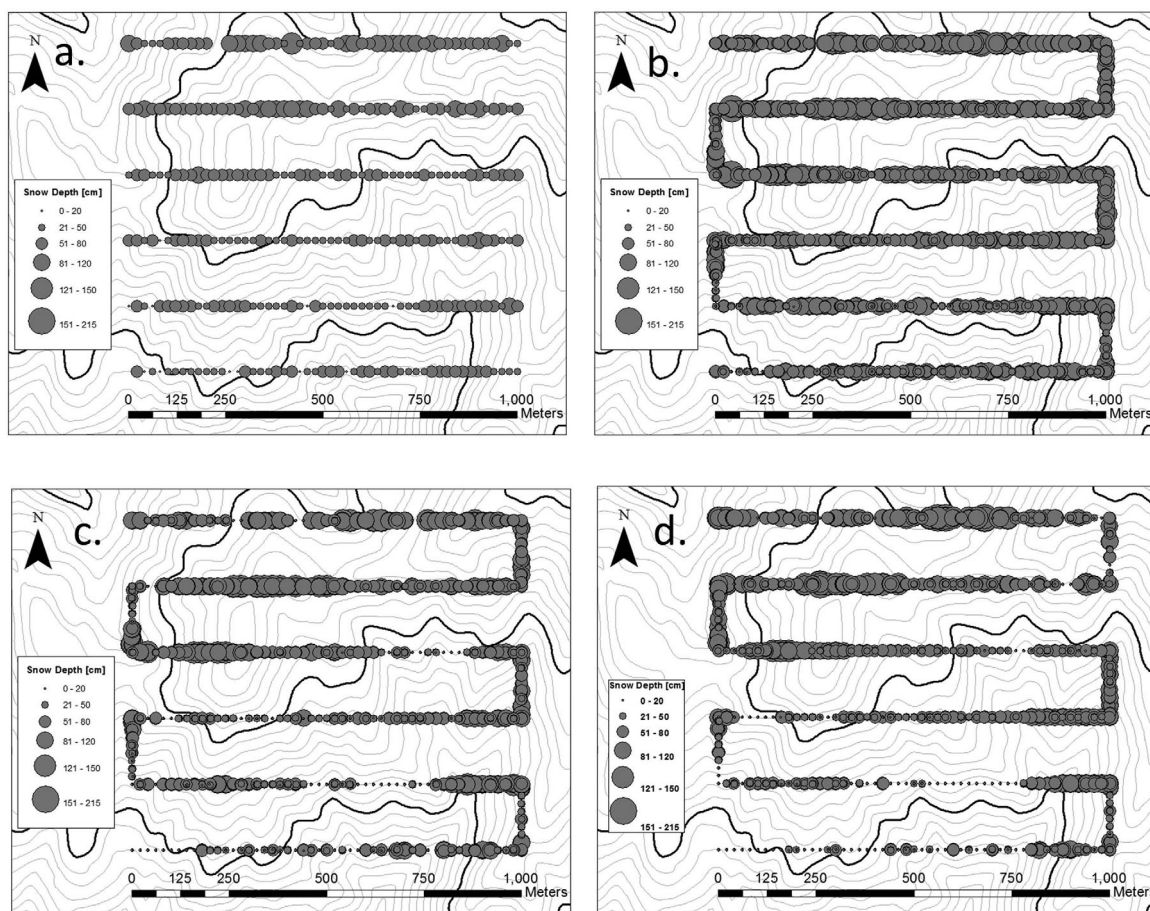


Figure 6. LDP grid snow depths on (a) 15 January 2010, (b) 19 February 2010, (c) 22 March 2010, and (d) 16 April 2010.

that the increasing correlation with aspect was not due to redistribution during storms, but was due to processes that occurred between storms, such as aspect-driven differential ablation. Wind redistribution, however, is indeed an important process in the DCEW, although to a lesser extent than the nearby Reynolds Creek Experimental Watershed [e.g., *Winstral and Marks, 2002*]. *Kormos [2013]*, for example, could not adequately simulate snow on the ground using a physically based snow accumulation model in the Treeline Watershed without incorporating a wind redistribution factor.

Results from Low Transect in the Treeline Watershed illustrate the combined influence of aspect-related insolation and wind effects on snow distribution. The orientation of the Treeline Watershed dictates that wind and insolation tend to have similar effects on snow distribution. Prevailing winds from the west and south deposit more snow on NE leeward aspects, while insolation preferentially ablates snow on SW aspects. The increasing correlation between aspect and snow depth through the season (Table 2), along with the evolving parameters of the variograms (Figure 11) suggest that wind redistribution is an early and persistent source of variability but the pattern it produces is amplified by insolation as the season advances. Although early season variations in snow depth at Low Transect were small (Figure 11), Student's *t* tests ($\alpha = 0.05$) confirm that mean snow depths on the northeast and southwest aspects were significantly different from each other on all sampling dates. The late-season variogram ranges or correlation lengths at Low Transect, between 53 and 46 m (Table 3), closely match hillslope lengths. Because maximum accumulation at Low Transect occurred in mid-January, we suggest that the continued evolution of aspect-dependent variability was predominately due to hillslope-scale insolation. Accumulated potential incoming solar radiation modeled for a 10 day period during the spring melt corresponds well with the observed snowmelt patterns (Figure 9f); supporting the suggestion that solar loading is the primary cause of mid- to late-season variability.

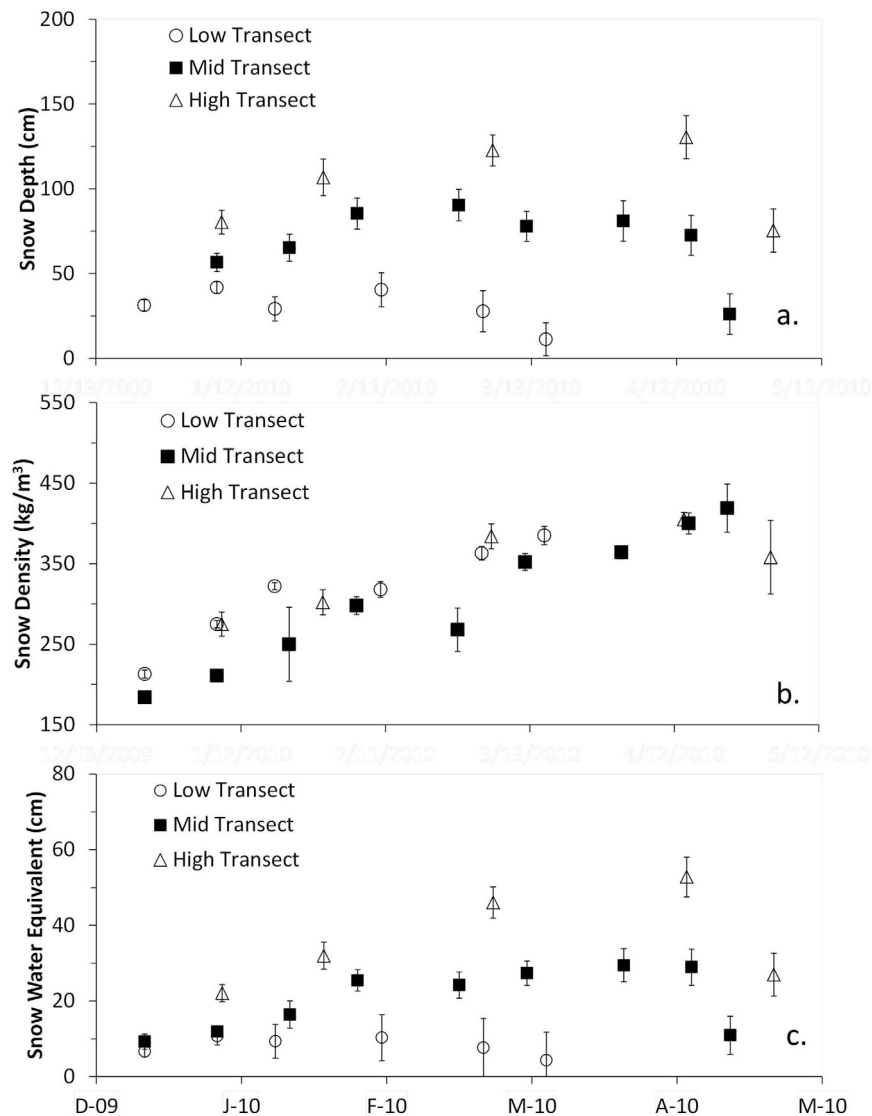


Figure 7. Mean values of (a) snow depth, (b) snow density, and (c) SWE at transect sites. Error bars are 1 standard deviation centered on the mean.

5.3. Canopy Density

Like aspect, canopy density impacts a suite of interacting processes that effect the accumulation and ablation of snow [Lundquist et al., 2013; Varhola et al., 2010]. Canopy cover intercepts falling snow [Hedstrom and Pomeroy, 1998] but also influences ablation by shading snow from solar radiation, acting as an emitter of longwave radiation and reducing wind speed [Link and Marks, 1999]. In the DCEW, there are apparent conflicts in the relationships between canopy density and snow at different scales. At the basin scale, forested sites held more late-season snow than open sites (Table 2). Conversely, low canopy density sections within the Mid Transect had deeper snow than did the high canopy density sections (Figure 10). The apparent conflict can be explained in two ways. First, at the basin scale, forested sites are related to other factors that also promote more snow: forested sites occur at higher elevations and on northerly aspects. Second, the effect of canopy density may be scale dependent. As canopy density decreases, the dominant role of forests may transition from reducing snowfall by interception and subsequent sublimation, to reducing snowmelt by shading.

Essentially, the basin scale analysis (Table 2) compares forested versus nonforested sites, whereas the Mid Transect analysis (Figure 10) compares relatively open versus relatively closed canopy sections within a

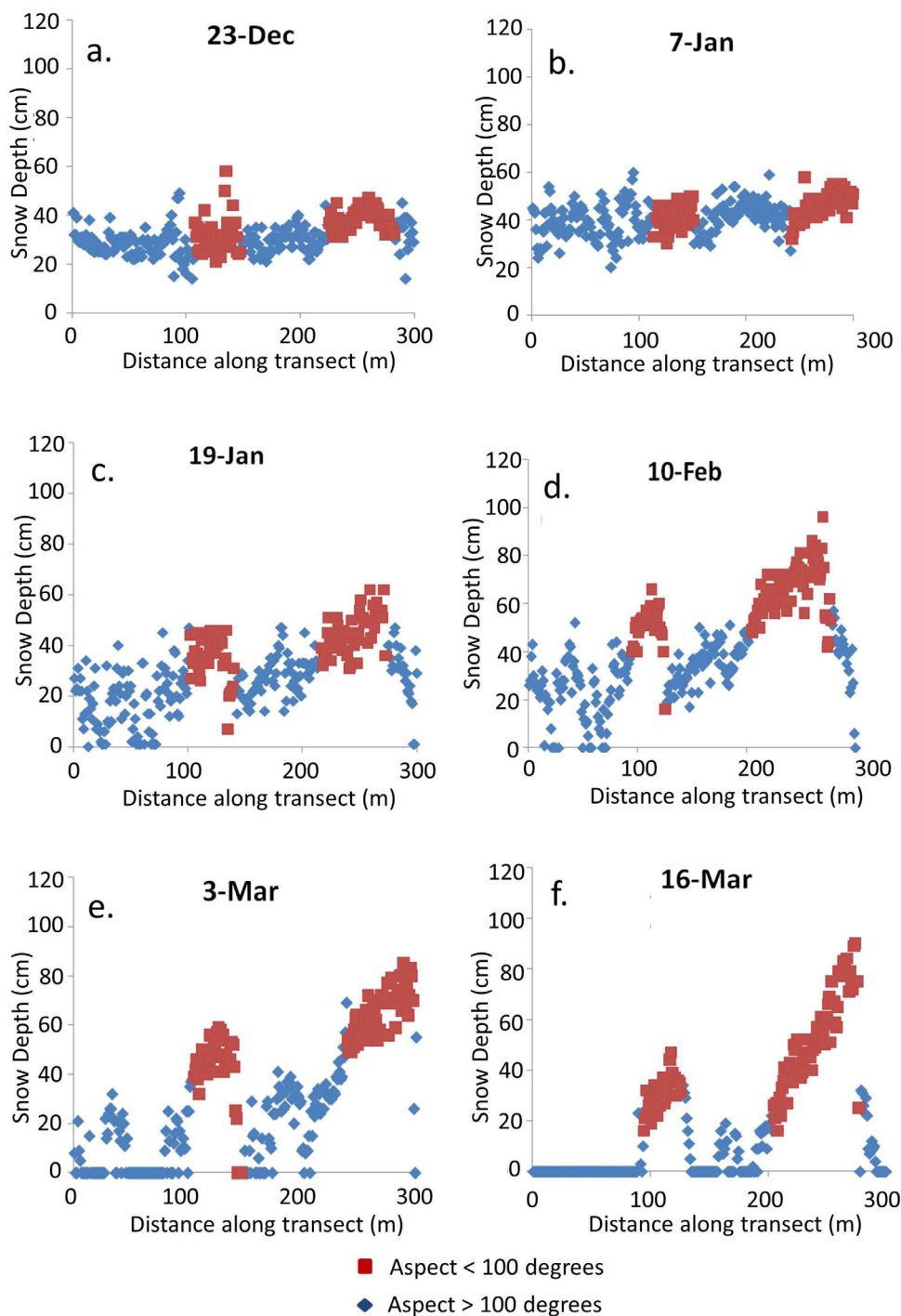


Figure 8. Snow depth in 2010 at the Low Transect on (a) 23 December, (b) 7 January, (c) 19 January, (d) 10 February, (e) 3 March, and (f) 16 March. Blue points are generally southeast-southwest facing, red points are generally northeast facing.

forested site. The differences are apparent in the variability in canopy density ranges at the two scales. Sixty percent of basin survey sites have canopy density values of 0, compared to only 15% within the Mid Transect (data not shown). The mean canopy density for the basin is 19%, compared to 51% within the Mid Transect. Additional studies are required to identify the canopy density range where forests transition from promoting less snow to more snow. Regardless, our findings at both basin and transect scales are consistent with existing literature [Lundquist et al., 2013; Veatch et al., 2009].

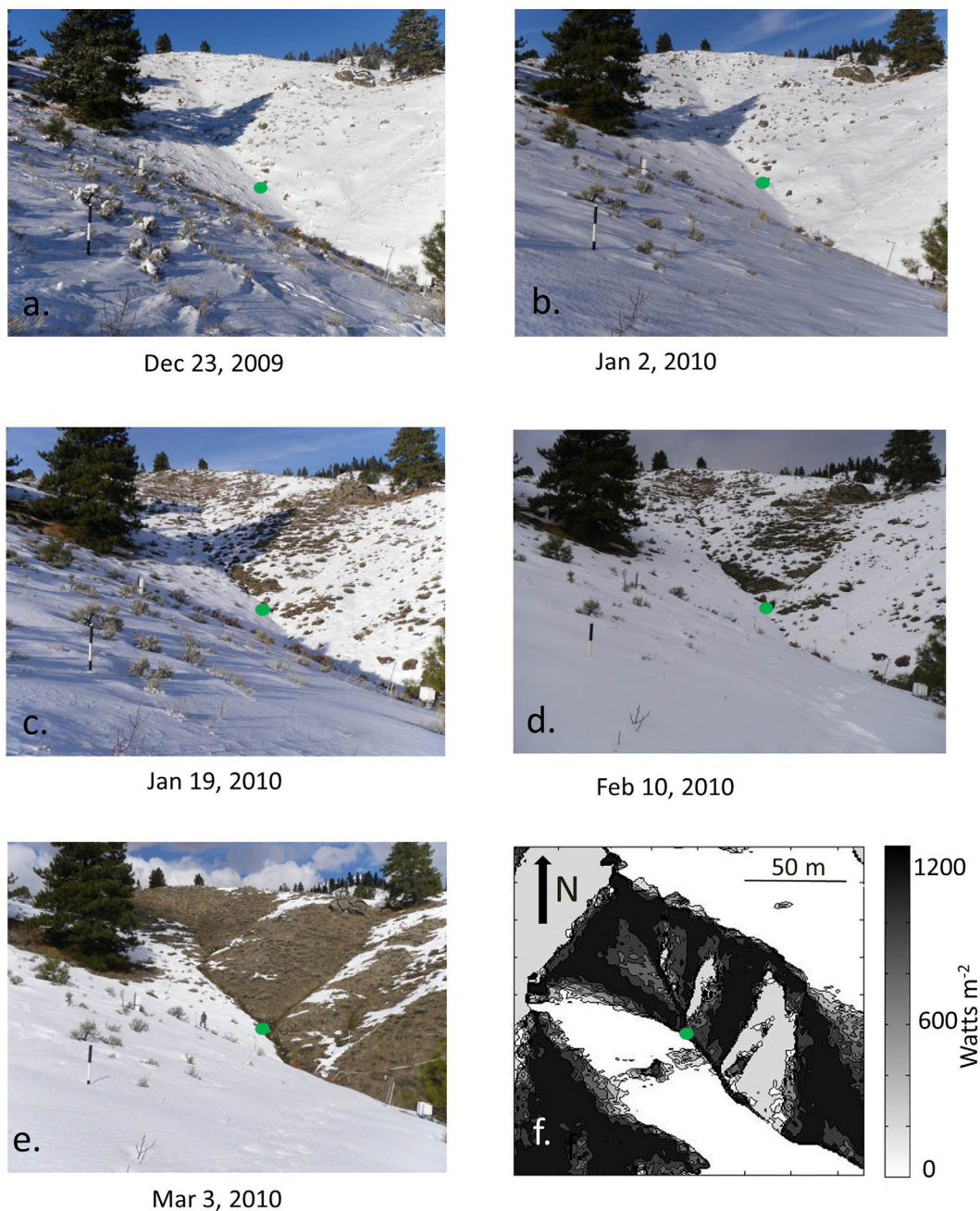


Figure 9. Time lapse images of the Treeline Watershed facing North. A 1 m marker with 25 cm increments is located in the left foreground. Note: The author sampling with the MagnaProbe in plot (e). Plot (f) illustrates modeled accumulated potential solar radiation for March 1 to March 10. Plot (f) is not scaled or oriented, but its relationship to plots (a)–(e) is clear from visual inspection.

The positive correlation between snow depth and canopy density at the basin scale agrees with the findings of *Lundquist et al.* [2013] who demonstrated that in areas with average winter temperatures $< -1^{\circ}\text{C}$, such as the DCEW, forested sites tend to retain snow longer due to enhanced ablation in open sites. The effect of interception under high canopy densities within forested sites agrees with the findings of *Veatch et al.* [2009], who showed that the deepest snow in forest stands resides under moderate canopy densities. At Mid Transect, this is most apparent in the early season (Figure 10a). In some instances, snow depth in high canopy density sections was approximately 50% lower than in low density sections. Similarly, a study in northern Idaho reported that approximately one third of snowfall was intercepted in Douglas Fir and

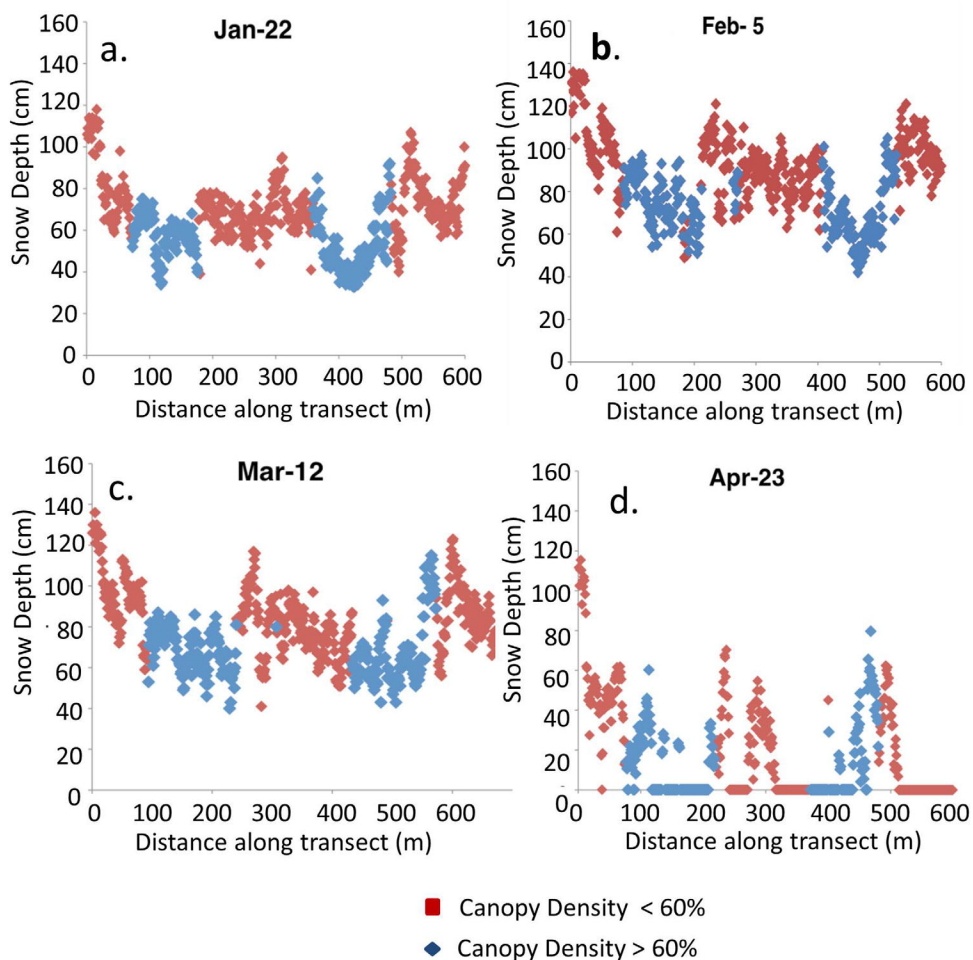


Figure 10. Snow depth in 2010 at Mid Transect on (a) 22 January, (b) 5 February, (c) 12 March, and (d) 23 April. Blue points have >60% canopy density and red points have <60% canopy density.

White Pine [Satterlund and Haupt, 1970]. The reduction in the correlation length through the season at the Mid Transect (Table 3) is likely related to the reduction in snow depth differences between high and low canopy density areas (Figures 10a–10d).

A premise of this paper is that improved understanding of the causes behind correlations between snow and terrain properties may help diagnose model performance issues. Although a full evaluation any particular model is beyond the scope of this paper, we compared our data to outputs of the Snow Data Assimilation System (SNODAS) of the US National Weather Service [Carroll et al., 2006]. SNODAS simulates snow properties for the Continental United States at a resolution of 1 km², several orders of magnitude greater than typical scales of SWE variability. We obtained SNODAS predictions of snow depth, density, and SWE for the duration of our study for each pixel within the DCEW from the National Operational Hydrologic Remote Sensing Center (www.nohrsc.gov). At LDP grid, SNODAS consistently under predicted snow depth and increasingly under predicted snow density throughout the season, resulting in increasing under prediction of SWE (Figure 5). SNODAS generally under predicted SWE at the basin scale as well (Figure 4). Careful inspection of Figure 5c illustrates that SNODAS generally captured increases in SWE well. This suggests that SNODAS generally performs well in describing the processes affecting accumulation, such as elevation-induced differential accumulation, and interception by forest canopy. However, SNODAS generally overpredicted midwinter SWE reductions. Note that SNODAS predicted a substantial decrease in SWE in early January (Figure 5c) during the same time period when observations show incipient divergence between the precipitation-elevation gradient and the SWE-elevation gradient (Figure 12). This suggests that SNODAS

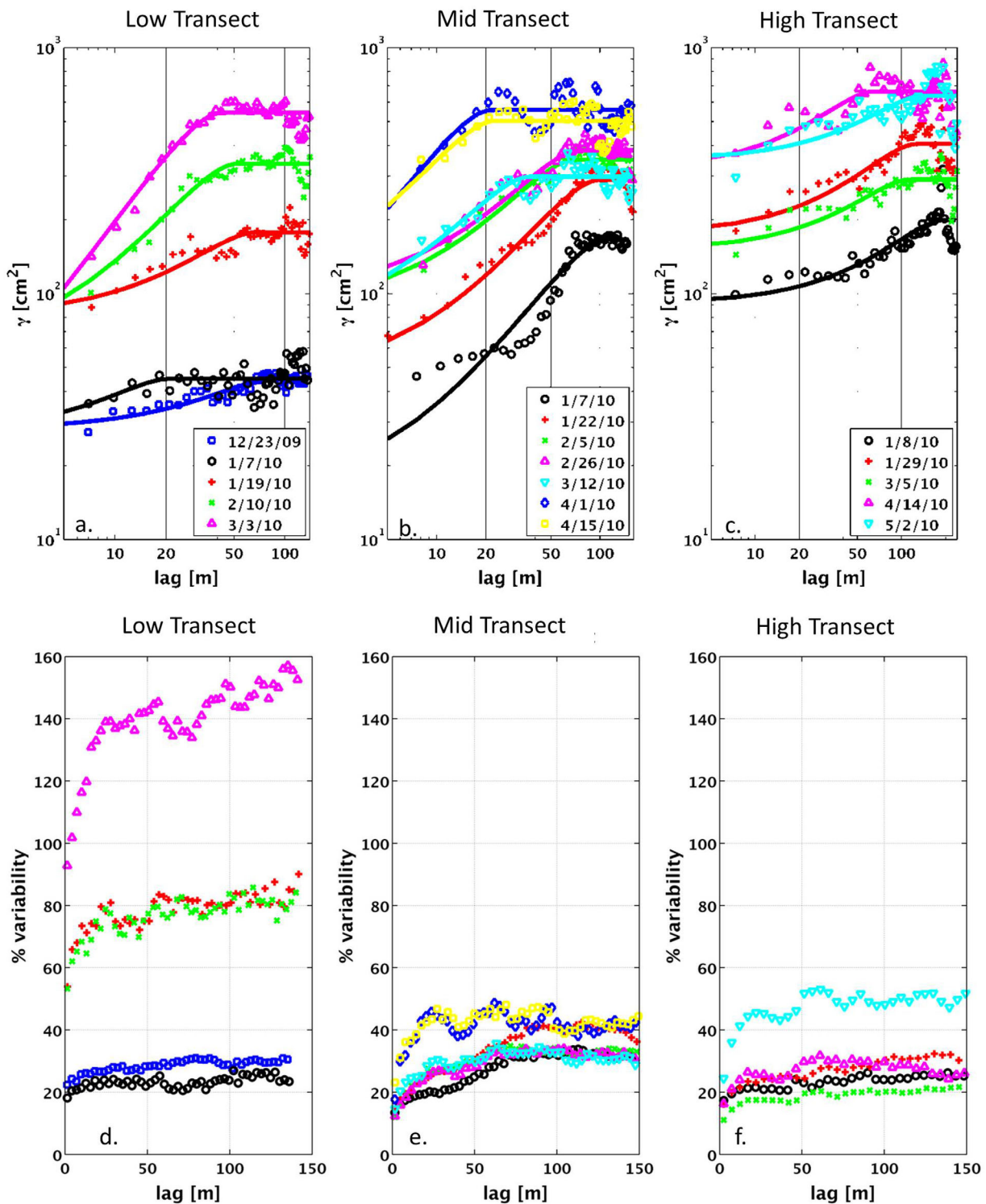


Figure 11. (a, b, c) Variograms and (d, e, f) pairwise relative semivariance (relative variability) plots for Low Transect, Mid Transect, and High Transect.

may have errantly propagated the ablation that occurred at elevations represented by the Low Transect in early January to elevations closer to the LDP grid, when in fact LDP grid experienced minimal ablation. Because the effect of canopy density on differential ablation is not strong until later in the season (Table 2), we look to the effect of aspect-induced insolation. The LDP grid and corresponding SNODAS pixel are

Table 3. Variogram Model Parameters

Date/Location	Nugget	Range	Range	Range	Sill	Sill	Sill
	(cm ²)	(m)	+ error	- error	(cm ²)	+ error	- error
<i>Treeline Transect</i>							
23 Dec 2009	20	35	63	18	42	10	5
7 Jan 2010	20	12	6	9	42	6	5
19 Jan 2010	45	37	22	8	156	17	21
10 Feb 2010	50	53	16	16	326	58	43
3 Mar 2010	40	47	7	13	569	79	95
16 Mar 2010	0	46	24	15	588	75	104
<i>Lower Deer Point Transect</i>							
23 Dec 2009	45	66	150	44	306	150	75
7 Jan 2010	25		NA	NA		NA	NA
22 Jan 2010	35	133	167	133	360	NA	NA
5 Feb 2010	35	64	13	24	351	39	37
26 Feb 2010	54	75	12	16	403	40	39
12 Mar 2010	47	37	26	8	314	30	20
1 Apr 2010	45	23	4	4	568	63	56
15 Apr 2010	70	26	6	7	531	54	48
23 Apr 2010	70	35	9	10	556	72	69
<i>Upper Dry Creek Transect</i>							
8 Jan 2010	45	32	104	14	108	42	23
29 Jan 2010	85	47	70	8	373	98	40
5 Mar 2010	60	33	95	16	275	80	26
14 Apr 2010	90	25	34	9	655	103	77
2 May 2010	60	26	16	6	550	43	43
<i>Lower Deer Pixel</i>							
15 Jan 2010	175	150	NA	NA	400	NA	NA
19 Feb 2010	60	106	46	26	520	44	33
22 Mar 2010	70	258	40	25	1050	56	52
15 Apr 2010	60	250	47	136	1190	73	77

dominantly south facing, but substantial subpixel variability exists. If SNODAS assigns a southerly aspect to the entire model pixel, the model will likely over predict the amount of melt generated by solar radiation. While Clow *et al.* [2012] demonstrated that adjusting for the effects of wind on snow distribution can improve the performance of SNODAS in high alpine environments, our observation suggests that subgrid distribution of insolation should be considered [Walters, 2013]. Both cases demonstrate that as coarse resolution models necessarily simplify processes in order to reduce complexity, it is essential to retain adequate representation of processes known to be locally important. Statistical downscaling using terrain parameters may be one possible approach to improving performance in complex terrain.

6. Conclusions

Causes behind correlations between snow and terrain properties can be ambiguous, particularly when correlations are based on one-time synoptic surveys. Repeated transect snow surveys distributed along an elevation gradient provided insight into the evolution of snow variability and helped explain how correlations arise. The variance of snow depth (variogram sills) increased consistently at each transect while the correlation length (variogram ranges) generally decreased as the season

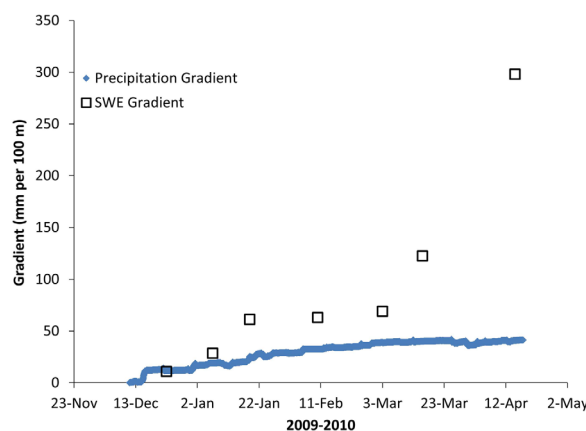


Figure 12. Gradients of cumulative precipitation over elevation between Treeline meteorological station and Bogus Basin SNOTEL (blue triangles), and SWE on the ground over elevation between Low Transect and High Transect (open black squares). SWE gradients are derived from Figure 7.

progressed. Trends are not as consistent in ranges as in sills. However, late-season correlation lengths compare favorably to dominant local terrain features such as hillslope lengths. This finding suggests that as the season progresses, small sources of variability gain strength, possibly due to positive feedback mechanisms, compared to larger scale patterns. In the DCEW, elevation was the strongest correlate with snow depth at the basin scale. Elevation-induced differential precipitation imposes a persistent source of variability at the basin scale. The precipitation-elevation gradient, however, is not sufficient to explain how late-season snow water equivalent (SWE) changes with elevation. Earlier and more frequent ablation at lower elevations, particularly on south and west aspects steepens the SWE-elevation gradient. Aspect and canopy density impose variability at smaller scales. Correlations with aspect are primarily controlled by differences in solar loading causing differential ablation. Redistribution by wind, however, is important early in the season. As ablation-induced variability increases through the season, redistribution by wind during storms has a relatively smaller impact on the variability of SWE on the ground. Forested sites hold more snow than nonforested sites at the basin scale due to differences in ablation processes, while areas under relatively open canopies within forested sites hold more snow than areas under relatively closed canopies due to interception. However, as the season progresses energetic differences between open and covered areas within forested sites cause differences induced by interception to diminish. Results of this study can help determine which accumulation and ablation processes must be represented explicitly and which can be parameterized in models of snow dynamics, and may provide insight into the necessary spatial and temporal model resolutions.

The effects of forest canopy in the DCEW are scale dependent. When canopy spacing is large enough so that sites are characterized as forested or nonforested, enhanced ablation in nonforested areas results in increasingly less snow through the season relative to forested areas. Conversely, within forested areas, sections under dense canopy cover hold less snow due to interception than do sections under moderate canopy cover. As ablation commences, however, the effect of interception diminishes.

Acknowledgments

This research was supported in part by grants from the National Science Foundation (CBET-0854522, EAR-0943710), the National Atmospheric and Oceanic Administration (NA08NWS4620047), and NASA (NNX10AN30A, NNX10AO02G). All data are freely available by contacting the corresponding author by email.

References

- Aishlin, P., and J. P. McNamara (2011), Bedrock infiltration and mountain block recharge accounting using chloride mass balance, *Hydrological Processes*, 25(12), 1934–1948.
- Anderton, S. P., S. M. White, and B. Alvera (2004), Evaluation of spatial variability in snow water equivalent for a high mountain catchment, *Hydrological Processes*, 18(3), 435–453.
- Blöschl, G., R. Kirnbauer, and D. Gutknecht (1991), Distributed snowmelt simulations in an alpine catchment: 1. Model evaluation on the basis of snow cover patterns, *Water Resour. Res.*, 27(12), 3171–3179.
- Carroll, T. R., D. W. Cline, C. Olheiser, A. Rost, A. Nilsson, C. Bovitz, and L. Li (2006), NOAA's national snow analysis, paper present at 74th Annual Meeting of the Western Snow Conference, Las Cruces, N. M.
- Clark, M. P., J. Hendrikx, A. G. Slater, D. Kavetski, B. Anderson, N. J. Cullen, T. Kerr, E. O. Hreinnsson, and R. A. Woods (2011), Representing spatial variability of snow water equivalent in hydrologic and land-surface models: A review, *Water Resour. Res.*, 47, W07539, doi:10.1029/2011WR010745.
- Clow, D. W., L. Nanus, K. L. Verdin, and J. Schmidt (2012), Evaluation of SNODAS snow depth and snow water equivalent estimates for the Colorado Rocky Mountains, USA, *Hydrological Processes*, 26(7), 2583–2591.
- Deems, J. S., S. R. Fassnacht, and K. J. Elder (2008), interannual consistency in fractal snow depth patterns at two Colorado mountain sites, *J. Hydrometeorol.*, 9(5), 977–988.
- Dixon, D., S. Boon, and U. Silins (2013), Watershed-scale controls on snow accumulation in a small montane watershed, southwestern Alberta, Canada, *Hydrological Processes*, 28(3), 1294–1306.
- Eiriksson, D., M. Whitson, C. H. Luce, H. P. Marshall, J. Bradford, S. G. Benner, T. Black, H. Hetrick, and J. P. McNamara (2013), An evaluation of the hydrologic relevance of lateral flow in snow at hillslope and catchment scales, *Hydrological Processes*, 27(5), 640–654.
- Elder, K., J. Dozier, and J. Michaelsen (1991), Snow accumulation and distribution in an alpine watershed, *Water Resour. Res.*, 27(7), 1541–1552.
- Elder, K., W. Rosenthal, and R. E. Davis (1998), Estimating the spatial distribution of snow water equivalence in a montane watershed, *Hydrological Processes*, 12(1011), 1793–1808.
- Gillan, B. J., J. T. Harper, and J. N. Moore (2010), Timing of present and future snowmelt from high elevations in northwest Montana, *Water Resour. Res.*, 46, W01507, doi:10.1029/2009WR007861.
- Gray, D. M., and D. H. Male (1981), *Handbook of Snow: Principles, Processes, Management & Use*, Pergamon, Toronto, Canada.
- Hamlet, A. F., and D. P. Lettenmaier (2007), Effects of climate change on hydrology and water resources in the Columbia River Basin, *J. Am. Water Resour. Assoc.*, 35(6), 1597–1623.
- Harrison, W. (1986), Seasonal accumulation and loss of snow from a block mountain catchment in central Otago, *J. Hydrol. N. Z.*, 25(1), 1–17.
- Hedstrom, N., and J. Pomeroy (1998), Measurements and modelling of snow interception in the boreal forest, *Hydrological Processes*, 12(1011), 1611–1625.
- Homan, J. W., C. H. Luce, J. P. McNamara, and N. F. Glenn (2011), Improvement of distributed snowmelt energy balance modeling with MODIS-based NDSI-derived fractional snow-covered area data, *Hydrological Processes*, 25(4), 650–660.
- Homer, C. H., J. A. Fry, and C. A. Barnes (2012), The national land cover database, *U.S. Geological Survey Fact Sheet Rep.*, 2012–3020, 4 pp.
- Houghton, J. G. (1979), A model for orographic precipitation in the north-central Great Basin, *Mon. Weather Rev.*, 107(11), 1462–1475.

- Jost, G., M. Weiler, D. R. Gluns, and Y. Alila (2007), The influence of forest and topography on snow accumulation and melt at the watershed-scale, *J. Hydrol.*, *347*(1), 101–115.
- Kerr, T., M. Clark, J. Hendrikx, and B. Anderson (2013), Snow distribution in a steep mid-latitude alpine catchment, *Adv. Water Resour.*, *55*(0), 17–24.
- Kormos, P. R. (2013), Estimating deep percolation in the mountain real-snow transition zone, Ph.D. dissertation, Dep. of Geos., Boise State University, Boise, Idaho.
- Lapen, D. R., and L. W. Martz (1993), The measurement of two simple topographic indices of wind sheltering-exposure from raster digital elevation models, *Comput. Geosci.*, *19*(6), 769–779.
- Link, T. E., and D. Marks (1999), Point simulation of seasonal snow cover dynamics beneath boreal forest canopies, *J. Geophys. Res.*, *104*(D22), 27,841–27,857.
- Luce, C. H., and Z. A. Holden (2009), Declining annual streamflow distributions in the Pacific Northwest United States, 1948–2006, *Geophys. Res. Lett.*, *36*, L16401, doi:10.1029/2009GL039407.
- Lundquist, J. D., S. E. Dickerson-Lange, J. A. Lutz, and N. C. Cristea (2013), Lower forest density enhances snow retention in regions with warmer winters: A global framework developed from plot-scale observations and modeling, *Water Resour. Res.*, *49*, 6356–6370, doi: 10.1002/wrcr.20504.
- Meromy, L., N. P. Molotch, T. E. Link, S. R. Fassnacht, and R. Rice (2012), Subgrid variability of snow water equivalent at operational snow stations in the western USA, *Hydrol. Processes*, *27*, 2383–2400, doi:10.1002/hyp.9355.
- Molotch, N. P., and R. C. Bales (2005), Scaling snow observations from the point to the grid element: Implications for observation network design, *Water Resour. Res.*, *41*, W11421, doi:10.1029/2005WR004229.
- Satterlund, D. R., and H. F. Haupt (1970), The disposition of snow caught by conifer crowns, *Water Resour. Res.*, *6*(2), 649–652.
- Scipión, D. E., R. Mott, M. Lehning, M. Schneebeli, and A. Berne (2013), Seasonal small-scale spatial variability in alpine snowfall and snow accumulation, *Water Resour. Res.*, *49*, 1446–1457, doi:10.1002/wrcr.20135.
- Shallcross, A. (2011), *LIDAR Investigations of Snow Distribution in Mountainous Terrain*, Boise State Univ., Boise, Idaho.
- Shook, K., and D. M. Gray (1998), Small-scale spatial structure of shallow snowcovers, *Hydrol. Processes*, *10*(10), 1283–1292.
- Smith, T. J., J. P. McNamara, A. N. Flores, M. M. Gribb, P. S. Aishlin, and S. G. Benner (2011), Small soil storage capacity limits benefit of winter snowpack to upland vegetation, *Hydrol. Processes*, *25*(25), 3858–3865.
- Tarboton, D., G. Blöschl, K. Cooley, R. Kirnbauer, and C. Luce (2000), Spatial snow cover processes at Kuhtai and Reynolds creek, in *Spatial Patterns in Catchment Hydrology: Observations and Modelling*, edited by G. Blöschl and R. Grayson, pp. 158–186, Cambridge Univ. Press, Cambridge, U. K.
- Trujillo, E., J. A. Ramirez, and K. J. Elder (2007), Topographic, meteorologic, and canopy controls on the scaling characteristics of the spatial distribution of snow depth fields, *Water Resour. Res.*, *43*, W07409, doi:10.1029/2006WR005317.
- Trujillo, E., J. A. Ramirez, and K. J. Elder (2009), Scaling properties and spatial organization of snow depth fields in sub-alpine forest and alpine tundra, *Hydrol. Processes*, *23*(11), 1575–1590.
- Varhola, A., N. C. Coops, M. Weiler, and R. D. Moore (2010), Forest canopy effects on snow accumulation and ablation: An integrative review of empirical results, *J. Hydrol.*, *392*(3–4), 219–233.
- Veatch, W., P. D. Brooks, J. R. Gustafson, and N. P. Molotch (2009), Quantifying the effects of forest canopy cover on net snow accumulation at a continental, mid-latitude site, *Ecohydrology*, *2*(2), 115–128.
- Walters, R. D. (2013), Transfer of snow information across the macro-to-hillslope-scale gap using a physiographic downscaling approach: Implications for hydrologic modeling in semiarid, seasonally snow-dominated watersheds, Department of Geosciences, Boise State University, Boise, Idaho.
- Webster, R., and M. A. Oliver (2001), *Geostatistics for Environmental Scientists*, John Wiley, N. Y.
- Williams, C. J., J. P. McNamara, and D. G. Chandler (2009), Controls on the temporal and spatial variability of soil moisture in a mountainous landscape: The signature of snow and complex terrain, *Hydrol. Earth Syst. Sci.*, *13*(7), 1325–1336.
- Winstral, A., and D. Marks (2002), Simulating wind fields and snow redistribution using terrain-based parameters to model snow accumulation and melt over a semi-arid mountain catchment, *Hydrol. Processes*, *16*, 3585–3603, doi:10.1002/hyp.1238.